รายงานวิจัยฉบับสมบูรณ์

โครงการการศึกษาโครงสร้างและหน้าที่ของตัวเร่งปฏิกิริยาซีโอไลต์

โดย ผศ. ดร. ศิริพร จึงสุทธิวงษ์

มิถุนายน 2552

สัญญาเลขที่ MRG5080088

รายงานวิจัยฉบับสมบูรณ์

โครงการการศึกษาโครงสร้างและหน้าที่ของตัวเร่งปฏิกิริยาซีโอไลต์

ผศ. ดร. ศิริพร จึงสุทธิวงษ์

ภาควิชาเคมี คณะวิทยาศาสตร์ มหาวิทยาลัยอุบลราชธานี

สนับสนุนโดยสำนักงานกองทุนสนับสนุนการวิจัย

Abstract

Project Code: MRG5080088

Project Title: A Systematic First-Principles Study of the Structure and Function of Bi - Functional Zeolite catalysts

Investigator: Asst. Prof. Siriporn Jungsuttiwong
Department of Chemistry, Faculty of Science, Ubon Ratchathani University

E-mail Address: jsiriporn_2000@yahoo.com

Project Period: 2 years

The structure and electronic properties of the Brønsted acid site in B, Al or Ga isomorphously substituted ZSM-5 zeolites were studied by using two different models. The first model is termed, “embedded ONIOM,” and is employed to include the long-range interactions of the zeolite lattice beyond 12T. The Madelung potentials were determined by improving optimized point charges to reproduce the infinite zeolitic lattice crystal. This improved method has been integrated into the ONIOM forming a new embedded ONIOM (E-ONIOM). We found that the OH distances and νOH of the acidic proton in zeolite obtained from both models can predict the trend of acid strength as: B-ZSM-5 < Ga-ZSM-5 < Al-ZSM-5, which is in very good agreement with the experimental sequence. Furthermore, the PA data calculated from E-ONIOM is also consistent with the experimental trend: B-ZSM-5 < Ga-ZSM-5 < Al-ZSM-5. It has, therefore, been demonstrated that our embedded ONIOM model provides accurate performance and can be one of the useful and affordable methods for future mechanistic studies involving petrochemical reactions.

Keywords: Embedded ONIOM, DFT, Isomorphous Substituted ZSM-5

Abstract

Project Code: MRG5080088

Project Title: A Systematic First-Principles Study of the Structure and Function of Bi - Functional Zeolite catalysts

Investigator: Asst. Prof. Siriporn Jungsuttiwong
Department of Chemistry, Faculty of Science, Ubon Ratchathani
University

E-mail Address: jsiriporn_2000@yahoo.com

Project Period: 2 years

The structure and electronic properties of the Brønsted acid site in B, Al or Ga isomorphously substituted ZSM-5 zeolites were studied by using quantum cluster and embedded ONIOM approaches. In the former approach, zeolites are modeled by 5T and 12T quantum clusters, where T represents a Si or Al atom. In the latter model, called “Embedded ONIOM”, the long-range interactions of the zeolite lattice beyond the12T quantum cluster is included via optimized point charges added to the ONIOM(B3LYP/6-31G(d,p):UFF). Inclusion of the extended zeolitic framework covering the nanocavity has an effect on the structure and adsorption properties. We found that the OH distances and νOH of the acidic proton in zeolite obtained from both models can predict the trend of acid strength as: B-ZSM-5 < Ga-ZSM-5 < Al-ZSM-5, which is in very good agreement with the experimental sequence. Furthermore, the PA data calculated from E-ONIOM is also consistent with the experimental trend: B-ZSM-5 < Ga-ZSM-5 < Al-ZSM-5. It has, therefore, been demonstrated that our embedded ONIOM model provides accurate performance and can be one of the useful and affordable methods for future mechanistic studies involving petrochemical reactions.

Keywords: Embedded ONIOM, DFT, Isomorphous Substituted ZSM-5

บทคัดย่อ

การศึกษาโครงสร้าง และสมบัติทางอิเล็กตรอน ของซีโอไลต์ 3 ชนิด ได้แก่ B-ZSM-5, Al-ZSM-5 และ Ga-ZSM-5 โดยใช้ระเบียบวิธีที่แตกต่างกัน 2 วิธี คือ “quantum cluster” และ “embedded-ONIOM” สำหรับวิธีแรกตัดเอาเฉพาะบริเวณที่เกิดปฏิกิริยาและบริเวณใกล้เคียงมาศึกษา โดยเปรียบเทียบ 2 แบบจำลอง ที่มีขนาดต่างกันคือ 5T และ 12T โดย T แทนตำแหน่งอะตอมของ Si หรือ Al สำหรับวิธีที่สองเป็นการรวมเอาโครงสร้างซีโอไลต์ที่ถูกตัดออกในวิธีแรก ซึ่งการไม่คิดค่าอันตรกิริยาของโครงสร้างที่ถูกตัดออกนั้นส่งผลกระทบต่อค่าพลังงาน และสมบัติต่างๆ ในการดูดซับ ผลการทดลองพบว่า เมื่อนำเอาโครงสร้างทั้งหมดของซีโอไลต์มาคำนวณ ความยาวพันธะ OH และค่าพลังงานในการสั่นของพันธะ OH ของซีโอไลต์มีแนวโน้มที่สอดคล้องกับที่ค่าวัดได้จากการทดลองมากกว่าวิธีแรก โดยแนวโน้มความแรงของกรดที่ได้จากการทดลอง และจากผลการคำนวณสอดคล้องกันคือ B-ZSM-5 < Ga-ZSM-5 < Al-ZSM-5 นอกจากนั้นเรายังได้ทำการคำนวณค่าพลังงานโปรตอนอัฟฟินิตี้ (PA) โดยใช้วิธีที่ถูกต้องมากกว่าที่กล่าวข้างต้น คือ “embedded-ONIOM” พบว่าแนวโน้มความแรงของกรด สอดคล้องกับการทดลองเป็นอย่างดี ดังนั้นวิธี “embedded-ONIOM” จึงเป็นวิธีที่มีประโยชน์ และเหมาะสมในการที่จะศึกษาปฏิกิริยาอื่นๆ ที่สำคัญ รวมไปถึงปฏิกิริยาที่ใช้ในปิโตรเคมีที่ใช้ซีโอไลต์เป็นตัวเร่งปฏิกิริยา

Characterization of Acidic Positions and Acidity in Isomorphous Substituted ZSM-5: Embedded DFT/UFF Approach

(Executive Summary)

The property of the isomorphously substituted zeolites has been focused because the heteroatoms help in fine-tuning the strength of the acid sites and introducing bifunctional features to zeolite catalyst. In this work, the structure and electronic properties of the Brønsted acid site in B, Al or Ga isomorphously substituted ZSM-5 zeolites were studied by using an ONIOM embedded approach with the B3LYP density functional theory. The E-ONIOM models consist of three layers. The center is quantum cluster, the UFF force field handles the next layer and the outermost layer of the model is represented by a set of explicit and optimized charges to perfectly describe the infinite zeolite framework. The measure for determining of the acidity is the adsorption energy of NH_3 showed that the acid strength of the substituted ZSM-5 increases in the sequence: B–ZSM-5 < Ga–ZSM-5 < Al–ZSM-5, which is in good agreement with experimental results. The interaction of NH_3 with the Brønsted acid site indicated that NH_3 becomes protonated in contact with the zeolite cluster and the configurations in which the protonated NH_3 interacts with two lattice oxygen atoms are favored energetically. In addition, the calculated adsorption energy of NH_3 on Al–ZSM-5 is comparable with the experimental data. This indicates that the effects of Madelung potential due to atoms outside the quantum cluster by using our E-ONIOM method are essential to be taken into account. Furthermore the results show a prospective trend to predict properties of metal substituted zeolites which a special emphasis on Bronsted acid strength of zeolites.

Introduction

Since the introduction of synthetic zeolites as catalysts in fluid catalytic cracking of heavy petroleum distillates in 1962, catalysis has become the single most important application of zeolites in terms of financial impact. Driven by the potential economic impact, progress in zeolite catalysis has focused largely on the synthesis, post-synthesis modification, physio-chemical characterization and testing. Much less has been achieved in improving our fundamental understanding of the structure and functions of zeolites and their catalytic roles. This is indicated by the fact that there are a very large number of zeolite topologies known today yet only a very limited number of such zeolites are actually used in applications [1-11]. Fundamental molecular-level understanding of structure-function relationships of the catalytic activity of zeolites and mechanisms of reactions at the active sites will have significant impacts on catalytic and process design and thus drastically improving the industrial competitive edge. The presence of Al replacing Si in zeolite structure generates bridging hydroxyl group so called "Brønsted acid site". Many of catalytic properties of zeolites can be directly related to this Brønsted acidity. In fact, heteroatoms such as B, Ga, Fe and Zn, etc. can be introduced into the framework of zeolite [12-18] by the replacement of Si atoms. Many of these studies were focused on predicting the acid strength of isomorphously substituted ZSM-5. The ability to vary the acidity of the catalyst is of importance in determining the extent and selectivity of catalytic process. In previous experimental results, mostly obtained by IR spectroscopy and TPD of NH_3, Chu and Chang [19] predicted that the Brønsted acidity of substituted ZSM-5 increases in the order B-ZSM-5 << Fe-ZSM-5 < Ga-ZSM-5 < Al-ZSM-5, indicating that the catalytic properties can be tuned for particular reaction. There have been many theoretical studies on zeolite structure and reactivity [20-22].

Despite numerous efforts both theoretically and experimentally in the last two decades, there are many fundamental questions regarding zeolite catalysis that are still not well understood. There remain large gaps in our current understanding of the nature of the active sites of zeolites and the mechanisms of reactions catalyzed by zeolites. Due to recent advances in computer technology and method development, computational quantum chemistry can significantly contribute to bridging these gaps. The property of the isomorphously substituted zeolites has been focused because the heteroatoms help in fine-tuning the strength of the acid sites and introducing bifunctional features to zeolite catalyst. In this work, the structure and electronic properties of the Brønsted acid site in B, Al or Ga isomorphously substituted ZSM-5 zeolites were studied by using an ONIOM embedded approach with the B3LYP density functional theory.

Computational Details

There are three different models that have been employed to study the isomorphously substituted zeolites. The first model is the small 5T cluster model (Figure 1) which are parts of the 10-membered ring of ZSM-5 zeolites, consisting of five tetrahedrally coordinated atoms (Si, Al). They were taken from the crystal structure of the ZSM-5 lattice [23].

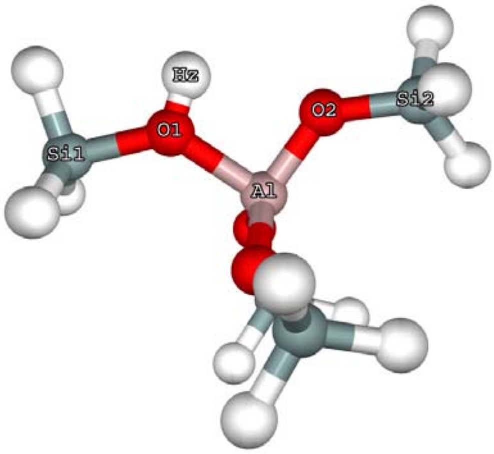

Figure 1. The 5T cluster model of H-ZSM-5

These rings are at the intersections of the channels and are accessible to the adsorbates. Hydrogen atoms were used to cap the dangling bonds. These capped hydrogen atoms are located along the direction of corresponding Si-O bonds. The resulting 5T clusters, Si4AlO4H13, have a total of 22 atoms. The second models are a larger 12T clusters, Si11AlO12H25, have a total of 49 atoms (Figure 2). They were selected to study the effects of unphysical interactions between small adsorbates and capped hydrogen atoms. These effects were remarkably observed in 5T cluster models. The T12 site was selected to represent the active site of ZSM-5 because it was found to be among the most stable sites for Al substitution [24-25] and this site provides sufficient space and can be accessed easily by small adsorbates. Most previous theoretical works have also chosen the T12 site as the Al substitution site for ZSM-5.

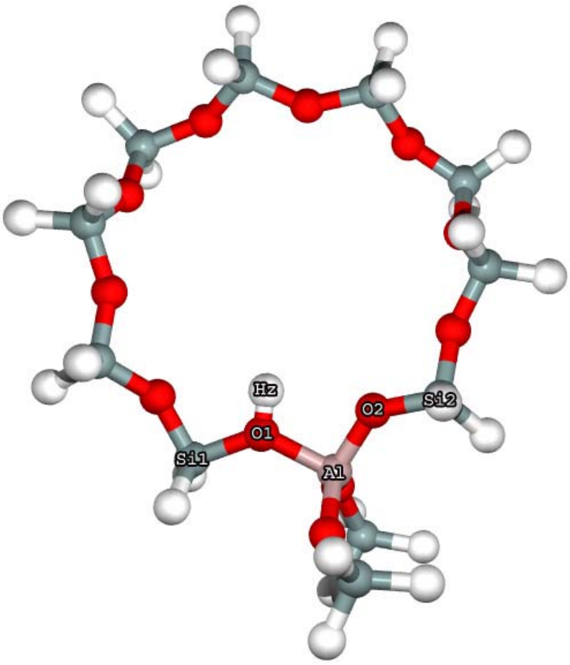

Figure 2. 12T-[Al]-ZSM-5 cluster model

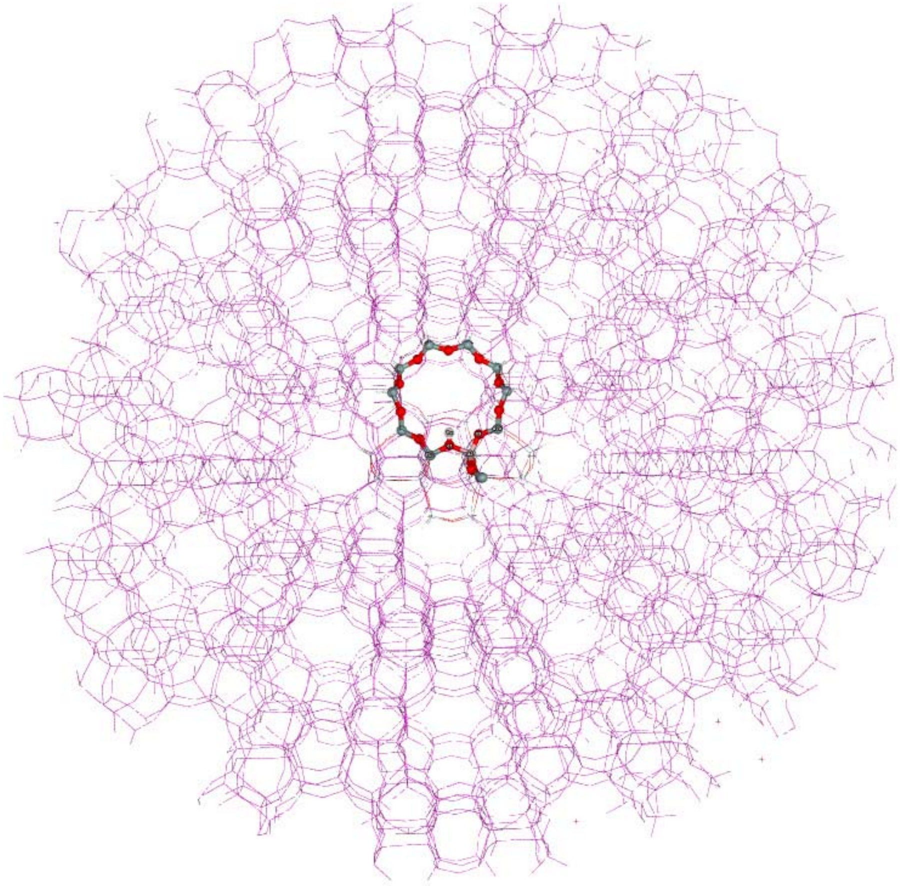

Figure 3. Embedded ONIOM12T-[Al]-ZSM-5 model

The third model is termed, “embedded ONIOM,” [26] and is employed to include the long-range interactions of the zeolite lattice beyond 12T (Figure 3). As point charges close to the quantum region can easily cause problems, we place our point charges only in a region defined by a minimal distance to the center of the quantum region and a maximal distance that determines the number of point charges. This finite number of point charges is further divided into an inner and an outer zone. Point charges in the inner zone (which might be a shell with a typical thickness of 5–10 Å and a few hundred point charges) are not optimized and have values one-half the formal charges of the zeolite atoms. Such “effective” charges Q_{Si} = +2 and Q_O = -1 are often used for a supermolecule such as zeolite and appear to be more realistic than the formal charges. The point charges in the outer region, which is a shell region immediately adjacent to the zone of the fixed charges, are optimized (typically there are a few thousand of them). We can define them by ΔQ, the vector of deviations from the values

$$Q'_{\text{outer}} = Q_{\text{outer}} + \Delta Q'' \qquad (1)$$

where ΔQ is derived in the following way. The electrostatic potential from the infinite crystal is calculated at the grid points using the Ewald method. The electrostatic potential from the zeolite cluster and from the point charges in both zones are then subtracted from it as follows:

$$V_{\text{outside}} = V_{\text{ewald}} - V_{\text{cluster}} - V_{\text{inner/outer}} \qquad (2)$$

We find the ΔQ that reproduces V_{outside} by solving the matrix of simultaneous linear equations:

$$A \cdot \Delta Q = V_{\text{outside}} \qquad (3)$$

where $V_{outside}$ is a column matrix with m rows if m is the number of grid points. A is the distance matrix having m rows, and n (the number of charges in the outer zone) columns. Its elements are defined as $A_{if} = 1/\left|R_i - R_j\right| \cdot R_i$. Ri is the position of grid point i, and Rj is the position of charge j. The Embedded ONIOM scheme has been shown in Figure 4.

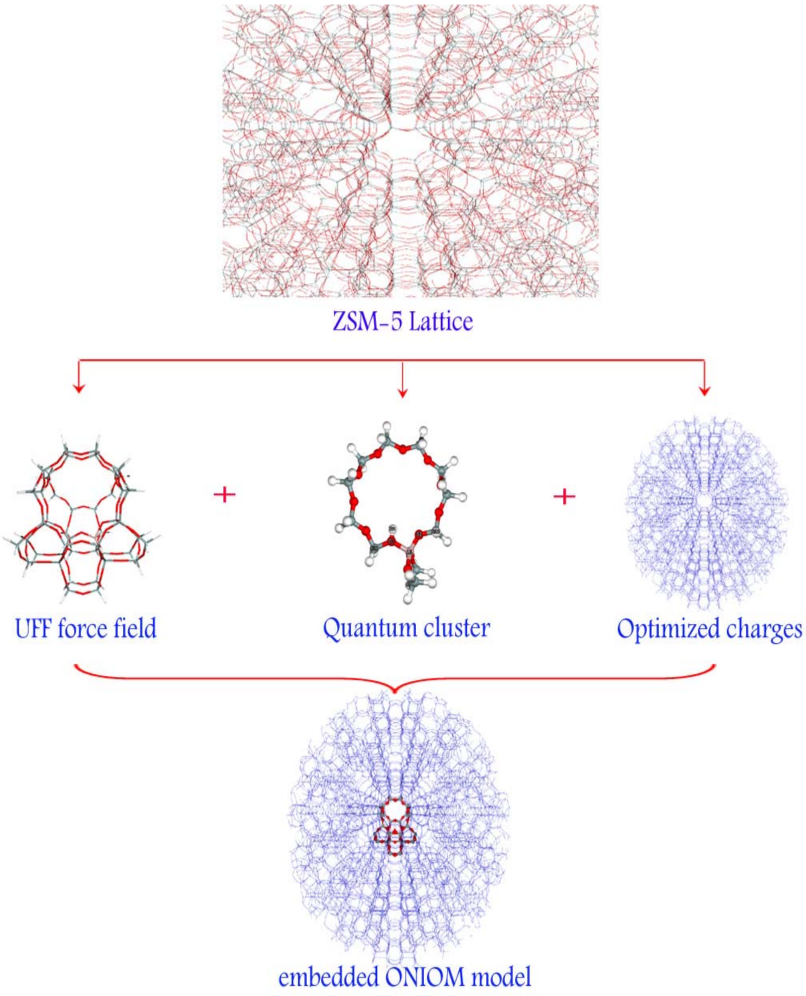

Figure 4. Embedded ONIOM Scheme

We now have a complete set of charges consisting of the point charges in the inner zone and the optimized point charges in the outer zone and their respective positions. This allows us to add the crystal potential to the quantum region. The system of equations described in Equation (3) also contains the four equations needed to guarantee the overall neutrality of charges and vanishing dipole moments along x, y, and z [27]. In all three models, the geometry optimizations were done at the B3LYP/ 6-31G (d, p) level. All calculations were performed using the GAUSSIAN 03 program [28].

Results and Discussion

a) The effect of lattice framework

In this study, in order to taking into account the effects of electron correlation, of large basis set, and of the BSSE correction in the determinations, the effects of lattice framework are included as well by using embedded ONIOM (E-ONIOM). We found that 5T cluster with fully optimized model at B3LYP/6-31G (d, p) level of theory, lead to structures that do not resemble experimental zeolite geometry, see Figure 5. The T – O1 distances are listed in table 1.

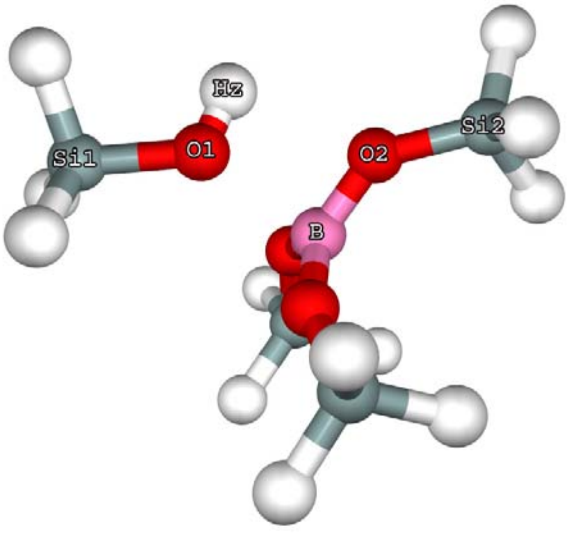

Figure 5. 5T-[B]-ZSM-5 cluster model

Table 1. The distances of T – O1 in isolated H-ZSM-5 with B3LYP/6-31G (d, p) level of theory.

Model	**Al – O1**	**B – O1**	**Ga – O1**
5T Cluster,	185.60	207.16	193.22
12T Cluster	183.98	204.57	191.61
12T E-ONIOM	179.40	176.88	187.46

However, when we included Madelung potential which determined by improving optimized point charges to reproduce of the infinite zeolitic lattice crystal integrated into the ONIOM (E-ONIOM method), the optimized model with electron correlation and large basis set, B3LYP/6-31G (d, p), become more accurate, see Figure 6. Furthermore OH distances and of acidic proton in zeolite obtained from Embedded ONIOM models can predict the trend of acid strength as: B-ZSM-5 < Ga-ZSM-5 < Al-ZSM-5, which is in a very good agreement with experimental sequence as shown in table 2.

Table 2. The distanced of O – H in isolated H-ZSM-5 with B3LYP/6-31G (d, p) level of theory

Model	**Al**-ZSM-5	**B**-ZSM-5	**Ga**-ZSM-5	acidity
5T Cluster	96.80	96.45	96.83	B < Al < Ga
12T Cluster	96.98	96.66	97.01	B < Al < Ga
12T E-ONIOM	97.07	96.93	97.06	B < Ga < Al
Experimental sequence of acid strength		B-ZSM-5 < Ga-ZSM-5 < Al-ZSM-5		

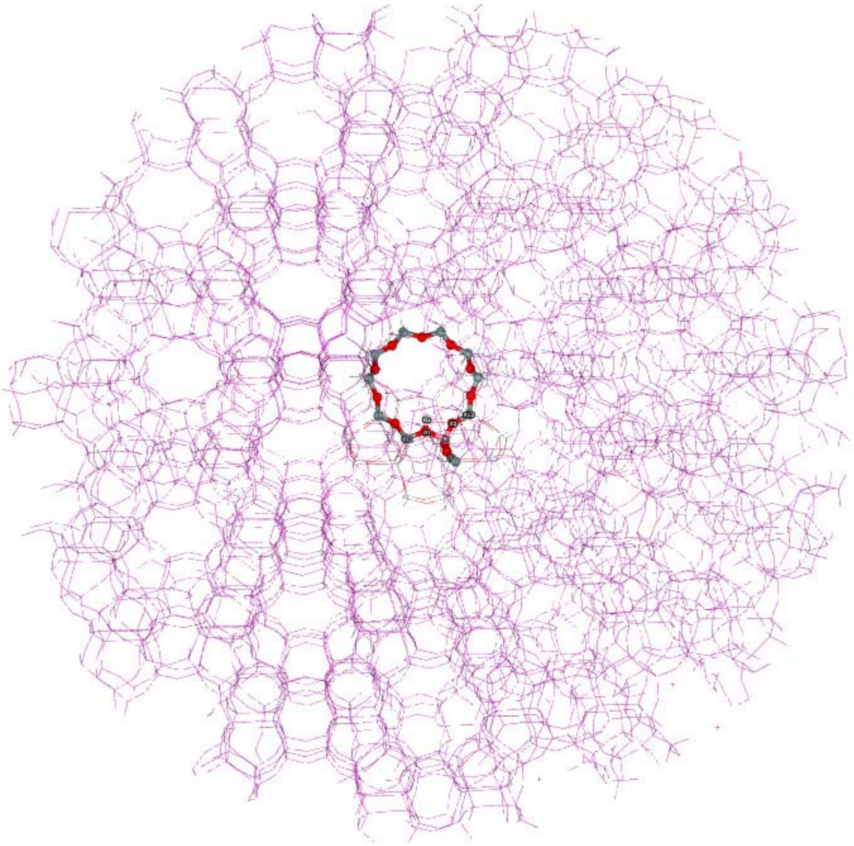

Figure 6. Embedded ONIOM12T-[B]-ZSM-5 model

b) Proton affinity of the substituted ZSM-5

Proton affinity (PA) can be served as a measure of the acid strength of ZSM-5. Indeed, direct experiments of the PA are not feasible. However, the data can be easily obtained from quantum calculation in which PA is considered as the energy required removing the acidic proton from the zeolite structure, and is calculated by equation (4)

$$PA = E_{ZO^-} - E_{ZOH} \tag{4}$$

Where E_{ZO^-} and E_{ZOH} are the energies of the deprotonated and the neutral clusters, respectively. It is obvious that the larger the PA, the weaker the acidity of the bridged hydroxyl group.

Table 3 PA and ν_{OH} calculated with B3LYP/6-31G (d, p) level of theory

Model	PA (kcal/mol)	
	12T Cluster	E-ONIOM 12T
B-ZSM-5	320.12	363.69
Ga-ZSM-5	313.36	362.31
Al-ZSM-5	308.98	357.68
Acidity sequence	B-ZSM-5 < Ga-ZSM-5 < Al-ZSM-5	

The predicted PA data listed in table 3 are calculated from 2 models, 12T cluster and E-ONIOM 12T giving the same trends of acid strength. These results are consistent with experimental trend: B-ZSM-5 < Ga-ZSM-5 < Al-ZSM-5. It is obvious that the larger the PA, the weaker the acidity of the bridged hydroxyl group. The PA data calculated from 3 models, 12T cluster, ONIOM 12T and E-ONIOM 12T giving the same trends of acid strength, which is consistent with experimental trend: B-ZSM-5 < Ga-ZSM-5 < Al-ZSM-5 as shown in table 4.

Table 4 The distances of O – H_z in isolated H-ZSM-5 with B3LYP/6-31G (d, p) level of theory.

Level of Theory	Al	B	Ga	Acidity trend
5T Cluster	96.80	96.45	96.83	B < Al < Ga
12T Cluster	96.98	96.66	97.01	B < Al < Ga
12T E-ONIOM	97.08	96.93	97.06	B < Ga < Al
ν_{OH} (cm^{-1}) calculated IR frequency	3604	3616	3608	B < Ga < Al

c) OH stretching frequency

It has been generally accepted that the stretching frequency of the OH bond, νOH, can be taken as an indicator of Brønsted acidity [29], lower wavenumber of νOH is related to weaker O – H bond strength and hence corresponds to stronger acid strength. The calculations are performed directly after the geometry optimization by B3LYP method with two different 12T models: 12T cluster and 12T E-ONIOM model. Positions of νOH are given in Table 5.

Table 5 The calculated ν_{OH} with B3LYP/6-31G (d,p) level of theory

ν_{OH} **(cm^{-1})**	**Acidity trend**	**T**		
		Al	**Ga**	**B**
12T E-ONIOM	B < Ga < Al	3604	3608	3616
12T Cluster	B < Al < Ga	3614	3612	3658
ν_{OH} [32] 8T cluster	B < Ga < Al	3816	3825	3830
ν_{OH} from IR [34]	B < Ga < Al	3610	3620	3725

The data calculated with 6-31G (d,p) should be scaled by 0.950 [30]. It is shown that the three different methods give the different acidity sequence. The ν_{OH} calculated from E-ONIOM 12T can provide trend corresponding to experimental result, our results also support the ν_{OH} in the region 3600 - 3700 cm^{-1} suggested by Chu et al. as fingerprint for Brønsted OH species. It is indicated that the DFT method with E-ONIOM 12T model is sufficient for this study.

d) Adsorption of NH_3 on ZSM-5

The Optimized adsorption structures of NH_3 on ZSM-5 are shown in Figures 7 – 8. Figure 7 represents the cluster model, and Figure 8 is the E-ONIOM model. Table 6 shows the energy of the adsorption of NH_3 on the acid site of the substituted ZSM-5 zeolites calculated by equation (5)

$$\Delta E_{ads} = E\ (\text{complex}) - E\ (\text{ZOH}) - E\ (NH_3) \qquad (5)$$

Table 6 Comparisons of Calculated Adsorption Energies of NH_3/Zeolite including BSSE at 6-311++G** basis set with Previous Theoretical and Experimental Results

	Level of Theory	**Cluster**	**Model**	**ΔE**
Al	B3LYP/6-31G (d,p)	12T	E-ONIOM	33.98
Al [33]	B3LYP/3-21G	8T	Cluster	50.7
Al [35]	experiment			33.5 – 35.6
Ga	B3LYP/6-31G (d,p)	12T	E-ONIOM	31.43
Ga [33]	B3LYP/3-21G	8T	Cluster	50.0
Ga [35]	experiment			34.52 – 36.90
B	B3LYP/6-31G (d,p)	12T	E-ONIOM	24.86
B [33]	B3LYP/3-21G	8T	Cluster	41.0

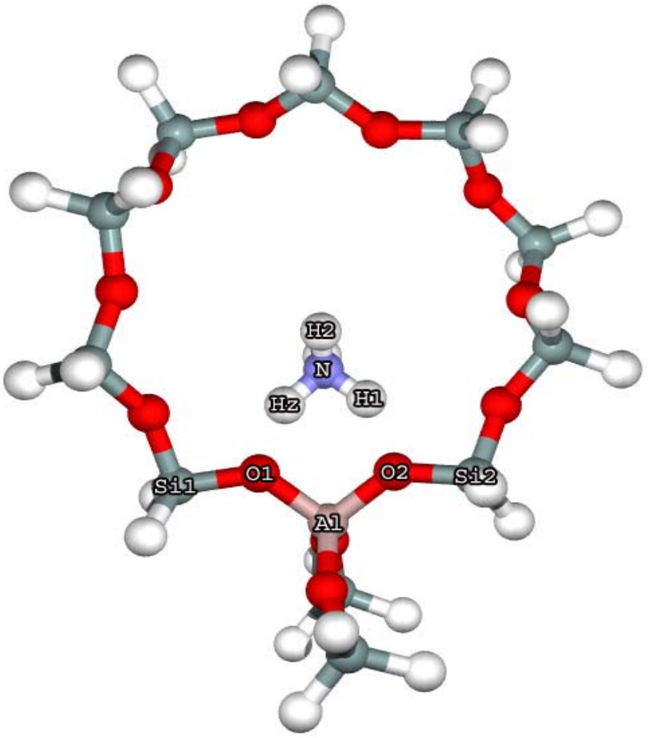

Figure 7. NH3 / 12T-[Al]-ZSM-5 model

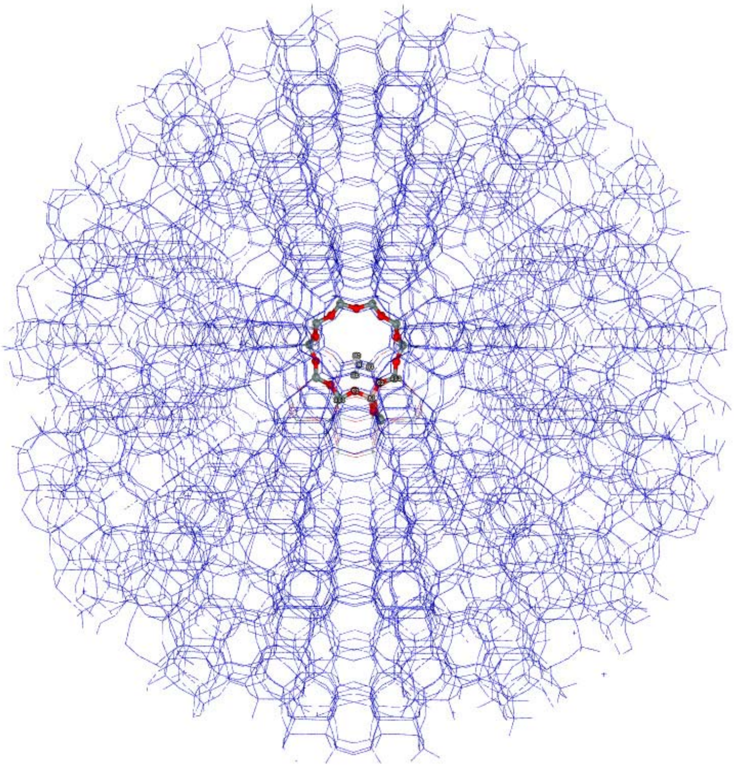

Figure 8. NH_3 / embedded ONIOM12T-[Al] ZSM-5 complex

It is shown that the relative acid strength predicted by adsorption energy of NH3 is consistent with that derived from PA and νOH of this paper, B–ZSM-5 < Ga–ZSM-5 < Al–ZSM-5. Moreover, the adsorption energies calculated with B3LYP/6-31G (d,p) for 12T E-ONIOM model are in better agreement with experimental results compared to those previous work [31-32].

Conclusions

The measure for determining of the acidity is the adsorption energy of NH_3 showed that the acid strength of the substituted ZSM-5 increases in the sequence: B–ZSM-5 < Ga–ZSM-5 < Al–ZSM-5, which is in good agreement with experimental results. The interaction of NH_3 with the Brønsted acid site indicated that NH_3 becomes protonated in contact with the zeolite cluster and the configurations in which the protonated NH_3 interacts with two lattice oxygen atoms are favored energetically. In addition, the calculated adsorption energy of NH_3 on Al–ZSM-5 is comparable with the experimental data. This indicates that the effects of Madelung potential due to atoms outside the quantum cluster by using our E-ONIOM method are essential to be taken into account. Furthermore the results show a prospective trend to predict properties of metal substituted zeolites which a special emphasis on Bronsted acid strength of zeolites.

References

1) Baburek, E.; Novakova, J. Applied Catalysis, A: General 2000, 190, 241.
2) Galindo, D. E.; Goncalves, M. J.; Ramirez-Corredores, M. M. Studies in Surface Science and Catalysis 2000, 130B, 1205.
3) Hochtl, M.; Kleber, C.; Jentys, A.; Vinek, H. Studies in Surface Science and Catalysis 2000, 130A, 377.
4) Ivanov, P.; Papp, H. Chemie, Ingenieur, Technik 2000, 72, 1213.
5) Ivanov, P.; Papp, H. Langmuir 2000, 16, 7769.
6) Pirngruber, G. D.; Seshan, K.; Lercher, J. A. Journal of Catalysis 2000, 190, 338.
7) Cerqueira, H. S.; Mihindou-Koumba, P. C.; Magnoux, P.; Guisnet, M. Industrial & Engineering Chemistry Research 2001, 40, 1032.
8) Davis, R. J. Journal of Catalysis 2003, 216, 396.
9) Kuznetsov, P. N. Journal of Catalysis 2003, 218, 12.
10) Aboul-Gheit, A. K.; Abdel-Hamid, S. M.; Awadallah, A. E. Oil, Gas (Hamburg, Germany) 2004, 30, 40.
11) Li, H.-Y.; Pu, M.; Liu, K.-H.; Zhang, B.-F.; Chen, B.-H. Chemical Physics Letters 2005, 404, 384.
12) Sauer, J. Chemical Review 1989, 89, 199.
13) Coudurier, G; Vedrine, J.C. Pure and Applied Chemistry 1986, 58, 1389.
14) Fricke, R.; Kosslick, H.; Lischke, M.; Chemical Review 2000, 100, 2303.
15) Yoshizawa, K.; Yumura, T.; Shiota, Y.; Yamabe, T. Bulletin of the Chemical Society of Japan 2000, 73, 29.
16) Bordiga, S.; Coluccia, S.; Lamberti, C.; Marchese, L.; Zecchina, A.; Boscherini, F.; Buffa, F.; Genoni, F.; Leofanti, G.; Vlaic, G.; Journal of Physical Chemistry, 1994, 98, 4125.
17) Dong, M.; Wang, J.; Sun, Y. Microporous and Mesoporouse Materials 2001, 43, 237.

18) Langenaeker, W.; Coussement, N.; Proft, De; Greerlings, P. Journal of Physical Chemistry, 1994, 98, 3010.
19) Chu, C. T. W.; Chang, C. D. Journal of Physical Chemistry, 1985, 89, 1569.
20) Alverado Swasigood, A. E.; Barr, M. K.; Hay, P. J.; Redondo, A. Journal of Physical Chemistry, 1991, 95, 10031.
21) Nicholas, J. B.; Winans, R. E.; Harrison, R. J.; Iton, L. E.; Curtiss, L. A.; Hopfinger, A. J. Journal of Physical Chemistry, 1992, 96, 7958.
22) White, J. C.; Hess, A. C. Journal of Physical Chemistry, 1993, 97, 8703.
23) Mortier, W. J.; Van den Bossche, E.; Uytterhoeven, J. B. Zeolites 1984, 4, 41.
24) Alvarado-Swaisgood, A. E.; Barr, M. K.; Hay, P. J.; Redondo, A. J. Phys. Chem. 1991, 95, 10031.
25) Derouane, E. G.; Fripiat, J. G. Zeolites 1985, 5, 165.
26) Injan, N., Pannorad N, Probst M, Limtrakul J. Int. J. Quantum. Chem. 2005, 105, 898-905.
27) Derenzo, S.E.; Klintenberg, M.K.; Weber, M.J., J. Chem. Phys. 2000, 112, 2074.
28) Frisch, M. J.; Trucks, G. W.; H. B. Schlegel, G. E. S.; Robb, M. A.; Cheeseman, J. R.; Zakrzewski, V. G.; Montgomery, J. A.; Stratmann, R. E.; Burant, J. C.; Dapprich, S.; Millam, J. M.; Daniels, A. D.; Kudin, K. N.; Strain, M. C.; Farkas, O.; Tomasi, J.; Barone, V.; Cossi, M.; Cammi, R.; Mennucci, B.; Pomelli, C.; Adamo, C.; Clifford, S.; Ochterski, J.; Petersson, G. A.; Ayala, P. Y.; Cui, Q.; Morokuma, K.; Malick, D. K.; Rabuck, A. D.; Raghavachari, K.; Foresman, J. B.; Cioslowski, J.; Ortiz, J. V.; Stefanov, B. B.; Liu, G.; Liashenko, A.; Piskorz, P.; Komaromi, I.; Gomperts, R.; Martin, R. L.; Fox, D. J.; Keith, T.; Al-Laham, M. A.; Peng, C. Y.; Nanayakkara, A.; Gonzalez, C.; Challacombe, M.; Gill, P. M. W.; Johnson, B. G.; Chen, W.; Wong, M. W.; Andres, J. L.; Head-Gordon, M.; Replogle, E. S.; Pople, J. A. Gaussian 98 (ReVision A.7).
29) O'Malley, P.J.; Dwyer, J. Journal of Physical Chemistry, 1988, 92, 3005.
30) Brand, H. V.; Curtiss, L.A.; and Iton, L.E., J. Phys. Chem. 1992, 96, 7725.
31) Yuan, S.P.; Wang, J.G.; Li, Y.W.; Peng, S.Y. Journal of Molecular Catalysis A: Chemical 2002, 178, 267.
32) Parrillo, D. J.; Lee, C. R.; Gorte, J. White, David, Farneth, W. E. J. Phys. Chem., 1995, 99, 8745.
33) Yuan, S.P.; Wang, J.G.; Li, Y.W.; Peng, S.Y. Journal of Molecular Catalysis A: Chemical 2002, 178, 267.
34) Chu, C.T.-W.; Kuehl, G.H.; Chang, C.D. J. Phys. Chem., 1985, 89, 1569.
35) Parrillo, D. J.; Lee, C. R.; Gorte, J. White, David,; Farneth, W. E. *J. Phys. Chem.*, **1995**, *99*, 8745.

Output จากโครงการวิจัยที่ได้รับทุนจาก สกว.

1. ผลงานตีพิมพ์ในวารสารวิชาการนานาชาติ (ระบุชื่อผู้แต่ง ชื่อเรื่อง ชื่อวารสาร ปี เล่มที่ เลขที่ และหน้า) หรือผลงานตามที่คาดไว้ในสัญญาโครงการ
   - อยู่ระหว่างการเตรียม Manuscript
2. ผลงานตีพิมพ์ในวารสารวิชาการในประเทศ การเสนอผลงานในที่ประชุมวิชาการ
   - 2.1 S. Jungsuttiwong, J. Lomratsiri and J. Limtrakul, **“Characterization of Acidic Positions and Acidity in Isomorphous Substituted ZSM-5: Embedded DFT/UFF and DFT Approaches”** in the Proceeding Pure and Applied Chemistry International Conference (PACCON2009), January 14-16, 2009, Faculty of Science, Naresuan University, Thailand. (Oral presentation)
   - 2.2 S. Jungsuttiwong and J. Lomratsiri, **“A systematic first-principles study of the structure and function of bi-functional zeolite catalysts”** 32th Congress on Science and Technology of Thailand, October 10-22, 2006, Queen Sirikit National Convention Center, Bangkok, Thailand. (Poster presentation)
   - 2.3 Jarun Lomratsiri and S. Jungsuttiwong, **“A systematic first-principles study of the structure and function of bi-functional zeolite catalysts”** The First International Conference on Science and Technology for Sustainable Development of the Greater Mekong Sub-region, August 15-16, 2006, Khonkaen University, Thailand. (Poster presentation)

Characterization of Acidic Positions and Acidity in Isomorphous Substituted ZSM-5: Embedded DFT/UFF Approach

S. Jungsuttiwong1[*], J. Limtrakul[2] and J. Lomratsiri[1]

[1] Chemistry Department, Faculty of Science, Ubon Ratchathani University, Warinchumrap,
Ubon Ratchathani 34190, Thailand

[2] Chemistry Department and NONOTEC Center of Excellence, Kasetsart University,
Bangkok 10900, Thailand

[*] Corresponding authors: Siriporn Jungsuttiwong (jsiripor@sci.ubu.ac.th)

APPENDIX

Abstract

The structure and electronic properties of the Brønsted acid site in B, Al or Ga isomorphously substituted ZSM-5 zeolites were studied by using two different models. The first model is termed, “embedded ONIOM,” and is employed to include the long-range interactions of the zeolite lattice beyond 12T. The Madelung potentials were determined by improving optimized point charges to reproduce the infinite zeolitic lattice crystal. This improved method has been integrated into the ONIOM forming a new embedded ONIOM (E-ONIOM). We found that the OH distances and νOH of the acidic proton in zeolite obtained from both models can predict the trend of acid strength as: B-ZSM-5 < Ga-ZSM-5 < Al-ZSM-5, which is in very good agreement with the experimental sequence. Furthermore, the PA data calculated from E-ONIOM is also consistent with the experimental trend: B-ZSM-5 < Ga-ZSM-5 < Al-ZSM-5. It has, therefore, been demonstrated that our embedded ONIOM model provides accurate performance and can be one of the useful and affordable methods for future mechanistic studies involving petrochemical reactions.

Keywords: Embedded ONIOM, DFT, Isomorphous Substituted ZSM-5

Introduction

Since the introduction of synthetic zeolites as catalysts in fluid catalytic cracking of heavy petroleum distillate in 1962, catalysis has become the single most important application of zeolites in terms of financial impact. Driven by the potential economic impact, progress in zeolite catalysis has focused largely on the synthesis, post-synthesis modification, physio-chemical characterization and testing. Much less has been achieved in improving our fundamental understanding of the structure and functions of zeolites and their catalytic roles. This is indicated by the fact that there are a very large number of zeolite topologies known today yet only a very limited number of such zeolites are actually used in applications [1-11]. Fundamental molecular-level understanding of structure-function relationships of the catalytic activity of zeolites and mechanisms of reactions at the active sites will have significant impacts on catalytic and process design and thus drastically improving the industrial competitive edge. The presence of Al replacing Si in zeolite structure generates bridging hydroxyl group so called "Brønsted acid site". Many of catalytic properties of zeolites can be directly related to this Brønsted acidity. In fact, heteroatoms such as B, Ga, Fe and Zn, etc. can be introduced into the framework of zeolite [12-18] by the replacement of Si atoms. Many of these studies were focused on predicting the acid strength of isomorphously substituted ZSM-5. The ability to vary the acidity of the catalyst is of importance in determining the extent and selectivity of catalytic process. In previous experimental results, mostly obtained by IR spectroscopy and TPD of NH_3, Chu and Chang [19] predicted that the Brønsted acidity of substituted ZSM-5 increases in the order B-ZSM-5 << Fe-ZSM-5 < Ga-ZSM-5 < Al-ZSM-5, indicating that the catalytic properties can be tuned for particular reaction. There have been many theoretical studies on zeolite structure and reactivity [20-22].

Despite numerous efforts both theoretically and experimentally in the last two decades, there are many fundamental questions regarding zeolite catalysis that are still not well understood. There remain large gaps in our current understanding of the nature of the active sites of zeolites and the mechanisms of reactions catalyzed by zeolites. Due to recent advances in computer technology and method development, computational quantum chemistry can significantly contribute to bridging these gaps. The property of the isomorphously substituted zeolites has been focused because the heteroatoms help in fine-tuning the strength of the acid sites and introducing bifunctional features to zeolite catalyst. In this work, the structure and electronic properties of the Brønsted acid site in B, Al or Ga isomorphously substituted ZSM-5 zeolites were studied by using an ONIOM embedded approach with the B3LYP density functional theory.

Computational Details

There are three different models that have been employed to study the isomorphously substituted zeolites. The first model is the small 5T cluster model (Figure 1) which are parts of the 10-membered ring of ZSM-5 zeolites, consisting of five tetrahedrally coordinated atoms (Si, Al). The resulting 5T clusters, Si4AlO4H13, have a total of 22 atoms. To investigate the cluster size effect as well as the effects of unphysical interactions between small adsorbates and capped hydrogen atoms, the second models, larger 12T clusters (Si11AlO12H25), have been chosen. The resulting 12T clusters, Si4AlO4H13, have a total of 49 atoms (Figure 2). These two models, (5T and 12T) were taken from the crystal structure of the ZSM-5 lattice [23]. Hydrogen atoms were used to cap the dangling bonds. These capped hydrogen atoms are located along the direction of corresponding Si-O bonds. The T12 site, which is located at the intersection of the straight and sinusoidal channels of ZSM-5, was selected to represent the active site of ZSM-5 because it was found to be among the most stable sites for Al substitution [24-25]. Moreover this site provides sufficient space and can be accessed easily by small adsorbates therefore it allows a significant interaction between the bridging OH and adsorbed molecules. Most previous theoretical works have also chosen the T12 site as the Al substitution site for ZSM-5.

The third model is termed, “embedded ONIOM,” [26] and is employed to include the long-range interactions of the zeolite lattice beyond 12T (Figure 3). As point charges close to the quantum region can easily cause problems, we place our point charges only in a region defined by a minimal distance to the center of the quantum region and a maximal distance that determines the number of point charges. This finite number of point charges is further divided into an inner and an outer zone. Point charges in the inner zone (which might be a shell with a typical thickness of 5–10 Å and a few hundred point charges) are not optimized and have values one-half the formal charges of the zeolite atoms. Such “effective” charges QSi = +2 and QO = -1 are often used for a supermolecule such as zeolite and appear to be more realistic than the formal charges. The point charges in the outer region, which is a shell region immediately adjacent to the zone of the fixed charges, are optimized (typically there are a few thousand of them). We can define them by ΔQ, the vector of deviations from the values

$$Q'_{outer} = Q_{outer} + \Delta Q'' \qquad (1)$$

where ΔQ is derived in the following way. The electrostatic potential from the infinite crystal is calculated at the grid points using the Ewald method. The electrostatic potential from the zeolite cluster and from the point charges in both zones are then subtracted from it as follows:

$$V_{outside} = V_{ewald} - V_{cluster} - V_{inner/outer}$$

(2)

We find the ΔQ that reproduces Voutside by solving the matrix of simultaneous linear equations:

$$A \cdot \Delta Q = V_{outside} \tag{3}$$

where Voutside is a column matrix with m rows if m is the number of grid points. A is the distance matrix having m rows, and n (the number of charges in the outer zone) columns. Its elements are defined as $A_{if} = 1/\left|R_i - R_j\right| \cdot R_i$. Ri is the position of grid point i, and Rj is the position of charge j. The Embedded ONIOM scheme has been shown in Figure 4. We now have a complete set of charges consisting of the point charges in the inner zone and the optimized point charges in the outer zone and their respective positions. This allows us to add the crystal potential to the quantum region. The system of equations described in Equation (3) also contains the four equations needed to guarantee the overall neutrality of charges and vanishing dipole moments along x, y, and z [27]. In all three models, the geometry optimizations were done at the B3LYP/ 6-31G (d, p) level. All calculations were performed using the GAUSSIAN 03 program [28].

Results and Discussion

a) The effect of lattice framework

In this study, in order to taking into account the effects of electron correlation, of large basis set, and of the BSSE correction in the determinations, the effects of lattice framework are included as well by using embedded ONIOM (E-ONIOM). We found that 5T cluster with fully optimized model at B3LYP/6-31G (d, p) level of theory, lead to structures that do not resemble experimental zeolite geometry, see Figure 5. The T – O1 distances are listed in table 1. However, when we included Madelung potential which determined by improving optimized point charges to reproduce of the infinite zeolitic lattice crystal integrated into the ONIOM (E-ONIOM method), the optimized model with electron correlation and large basis set, B3LYP/6-31G (d, p), become more accurate, see Figure 6. Furthermore OH distances and of acidic proton in zeolite obtained from Embedded ONIOM models can predict the trend of acid strength as: B-ZSM-5 < Ga-ZSM-5 < Al-ZSM-5, which is in a very good agreement with experimental sequence as shown in table 2.

b) Proton affinity of the substituted ZSM-5

Proton affinity (PA) can be served as a measure of the acid strength of ZSM-5. Indeed, direct experiments of the PA are not feasible. However, the data can be easily obtained from quantum calculation in which PA is considered as the energy required removing the acidic proton from the zeolite structure, and is calculated by equation (4)

$$PA = E_{ZO^-} - E_{ZOH} \tag{4}$$

Where E_{ZO^-} and E_{ZOH} are the energies of the deprotonated and the neutral clusters, respectively. It is obvious that the larger the PA, the weaker the acidity of the bridged hydroxyl group. The predicted PA data listed in table 2 are calculated from 2 models, 12T cluster and E-ONIOM 12T giving the same trends of acid strength. These results are consistent with experimental trend: B-ZSM-5 < Ga-ZSM-5 < Al-ZSM-5. It is obvious that the larger the PA, the weaker the acidity of the bridged hydroxyl group. The PA data calculated from 3 models, 12T cluster, ONIOM 12T and E-ONIOM 12T giving the same trends of acid strength, which is consistent with experimental trend: B-ZSM-5 < Ga-ZSM-5 < Al-ZSM-5 as shown in table 3.

c) OH stretching frequency

It has been generally accepted that the stretching frequency of the OH bond, νOH, can be taken as an indicator of BrØnsted acidity [29], lower wavenumber of νOH is related to weaker O – H bond strength and hence corresponds to stronger acid strength. The calculations are performed directly after the geometry optimization by B3LYP method with three different 12T models: cluster, ONIOM and E-ONIOM. Positions of νOH are given in Table 4. The data calculated with 6-31G (d,p) should be scaled by 0.950 [30]. It is shown that the three different methods give the different acidity sequence. The ν_{OH} calculated from E-ONIOM 12T can provide trend corresponding to experimental result, our results also support the ν_{OH} in the region 3600 - 3700 cm^{-1} suggested by Chu et al. as fingerprint for BrØnsted OH species. It is indicated that the DFT method with E-ONIOM 12T model is sufficient for this study.

d) Adsorption of NH_3 on ZSM-5

The Optimized adsorption structures of NH_3 on ZSM-5 are shown in Figures 7 – 8. Figure 7 represents the cluster model, and Figure 8 is the E-ONIOM model. Table 5 shows the energy of the adsorption of NH_3 on the acid site of the substituted ZSM-5 zeolites calculated by equation (5)

$$\Delta E_{ads} = E\ (complex) - E\ (ZOH) - E\ (NH_3) \qquad (5)$$

It is shown that the relative acid strength predicted by adsorption energy of NH3 is consistent with that derived from PA and νOH of this paper, B–ZSM-5 < Ga–ZSM-5 < Al–ZSM-5.

Moreover, the adsorption energies calculated with B3LYP/6-31G (d,p) for 12T E-ONIOM model are in better agreement with experimental results compared to those previous work [31-32].

Conclusions

The measure for determining of the acidity is the adsorption energy of NH_3 showed that the acid strength of the substituted ZSM-5 increases in the sequence: B–ZSM-5 < Ga–ZSM-5 < Al–ZSM-5, which is in good agreement with experimental results. The interaction of NH_3 with the Brønsted acid site indicated that NH_3 becomes protonated in contact with the zeolite cluster and the configurations in which the protonated NH_3 interacts with two lattice oxygen atoms are favored energetically. In addition, the calculated adsorption energy of NH_3 on Al–ZSM-5 is comparable with the experimental data. This indicates that the effects of Madelung potential due to atoms outside the quantum cluster by using our E-ONIOM method are essential to be taken into account. Furthermore the results show a prospective trend to predict properties of metal substituted zeolites which a special emphasis on Bronsted acid strength of zeolites.

Acknowledgments

This work was supported in part by grants from the Thailand Research Fund (TRF-CHE Research Grant for New Scholar), the Ubon Ratchathani University and NONOTEC Center of Excellence, Kasetsart University.

References

(1) Baburek, E.; Novakova, J. Applied Catalysis, A: General 2000, 190, 241.

(2) Galindo, D. E.; Goncalves, M. J.; Ramirez-Corredores, M. M. Studies in Surface Science and Catalysis 2000, 130B, 1205.

(3) Hochtl, M.; Kleber, C.; Jentys, A.; Vinek, H. Studies in Surface Science and Catalysis 2000, 130A, 377.

(4) Ivanov, P.; Papp, H. Chemie, Ingenieur, Technik 2000, 72, 1213.

(5) Ivanov, P.; Papp, H. Langmuir 2000, 16, 7769.

(6) Pirngruber, G. D.; Seshan, K.; Lercher, J. A. Journal of Catalysis 2000, 190, 338.

(7) Cerqueira, H. S.; Mihindou-Koumba, P. C.; Magnoux, P.; Guisnet, M. Industrial & Engineering Chemistry Research 2001, 40, 1032.

(8) Davis, R. J. Journal of Catalysis 2003, 216, 396.

(9) Kuznetsov, P. N. Journal of Catalysis 2003, 218, 12.

(10) Aboul-Gheit, A. K.; Abdel-Hamid, S. M.; Awadallah, A. E. Oil, Gas (Hamburg, Germany) 2004, 30, 40.

(11) Li, H.-Y.; Pu, M.; Liu, K.-H.; Zhang, B.-F.; Chen, B.-H. Chemical Physics Letters 2005, 404, 384.

(12) Sauer, J. Chemical Review 1989, 89, 199.

(13) Coudurier, G; Vedrine, J.C. Pure and Applied Chemistry 1986, 58, 1389.

(14) Fricke, R.; Kosslick, H.; Lischke, M.; Chemical Review 2000, 100, 2303.

(15) Yoshizawa, K.; Yumura, T.; Shiota, Y.; Yamabe, T. Bulletin of the Chemical Society of Japan 2000, 73, 29.

(16) Bordiga, S.; Coluccia, S.; Lamberti, C.; Marchese, L.; Zecchina, A.; Boscherini, F.; Buffa, F.; Genoni, F.; Leofanti, G.; Vlaic, G.; Journal of Physical Chemistry, 1994, 98, 4125.

(17) Dong, M.; Wang, J.; Sun, Y. Microporous and Mesoporouse Materials 2001, 43, 237.

(18) Langenaeker, W.; Coussement, N.; Proft, De; Greerlings, P. Journal of Physical Chemistry, 1994, 98, 3010.

(19) Chu, C. T. W.; Chang, C. D. Journal of Physical Chemistry, 1985, 89, 1569.

(20) Alverado Swasigood, A. E.; Barr, M. K.; Hay, P. J.; Redondo, A. Journal of Physical Chemistry, 1991, 95, 10031.

(21) Nicholas, J. B.; Winans, R. E.; Harrison, R. J.; Iton, L. E.; Curtiss, L. A.; Hopfinger, A. J. Journal of Physical Chemistry, 1992, 96, 7958.

(22) White, J. C.; Hess, A. C. Journal of Physical Chemistry, 1993, 97, 8703.

(23) Mortier, W. J.; Van den Bossche, E.; Uytterhoeven, J. B. Zeolites 1984, 4, 41.

(24) Alvarado-Swaisgood, A. E.; Barr, M. K.; Hay, P. J.; Redondo, A. J. Phys. Chem. 1991, 95, 10031.

(25) Derouane, E. G.; Fripiat, J. G. Zeolites 1985, 5, 165.

(26) Injan, N., Pannorad N, Probst M, Limtrakul J. Int. J. Quantum. Chem. 2005, 105, 898-905.

(27) Derenzo, S.E.; Klintenberg, M.K.; Weber, M.J., J. Chem. Phys. 2000, 112, 2074.

(28) Frisch, M. J.; Trucks, G. W.; H. B. Schlegel, G. E. S.; Robb, M. A.; Cheeseman, J. R.; Zakrzewski, V. G.; Montgomery, J. A.; Stratmann, R. E.; Burant, J. C.; Dapprich, S.; Millam, J. M.; Daniels, A. D.; Kudin, K. N.; Strain, M. C.; Farkas, O.; Tomasi, J.; Barone, V.; Cossi, M.; Cammi, R.; Mennucci, B.; Pomelli, C.; Adamo, C.; Clifford, S.; Ochterski, J.; Petersson, G. A.; Ayala, P. Y.; Cui, Q.; Morokuma, K.; Malick, D. K.; Rabuck, A. D.; Raghavachari, K.; Foresman, J. B.; Cioslowski, J.; Ortiz, J. V.; Stefanov, B. B.; Liu, G.; Liashenko, A.; Piskorz, P.; Komaromi, I.; Gomperts, R.; Martin, R. L.; Fox, D. J.; Keith, T.; Al-Laham, M. A.; Peng, C. Y.; Nanayakkara, A.; Gonzalez, C.; Challacombe, M.; Gill, P. M. W.; Johnson, B. G.; Chen, W.; Wong, M. W.; Andres, J. L.; Head-Gordon, M.; Replogle, E. S.; Pople, J. A. Gaussian 98 (ReVision A.7).

(29) O'Malley, P.J.; Dwyer, J. Journal of Physical Chemistry, 1988, 92, 3005.

(30) Brand, H. V.; Curtiss, L.A.; and Iton, L.E., J. Phys. Chem. 1992, 96, 7725.

(31) Yuan, S.P.; Wang, J.G.; Li, Y.W.; Peng, S.Y. Journal of Molecular Catalysis A: Chemical 2002, 178, 267.

(32) Parrillo, D. J.; Lee, C. R.; Gorte, J. White, David, Farneth, W. E. J. Phys. Chem., 1995, 99, 8745.

(33) Yuan, S.P.; Wang, J.G.; Li, Y.W.; Peng, S.Y. Journal of Molecular Catalysis A: Chemical 2002, 178, 267.

(34) Chu, C.T.-W.; Kuehl, G.H.; Chang, C.D. J. Phys. Chem., 1985, 89, 1569.

(35) Parrillo, D. J.; Lee, C. R.; Gorte, J. White, David,; Farneth, W. E. *J. Phys. Chem.*, **1995**, *99*, 8745.

Figure Captions

Figure 1: The 5T cluster model of H-ZSM-5.

Figure 2: 12T-[Al]- ZSM-5 cluster model.

Figure 3: Embedded ONIOM 12T – [Al] – ZSM-5 model.

Figure 4: Embedded ONIOM Scheme.

Figure 5: 5T – [B] – ZSM-5 cluster model.

Figure 6: Embedded ONIOM 12T – [B] – ZSM-5 model.

Figure 7: NH_3 / 12T – [Al] – ZSM-5 complex.

Figure 8: NH_3 / Embedded ONIOM – [Al] – ZSM-5 complex.

Figure 10: The characteristic vibrational modes of the bridged hydroxyl group.

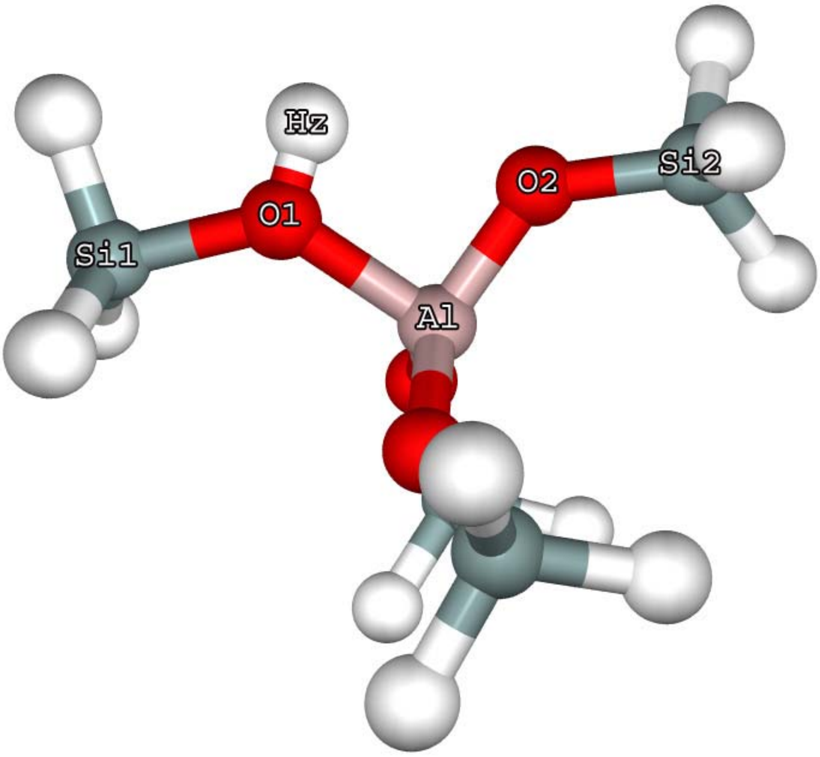

Figur

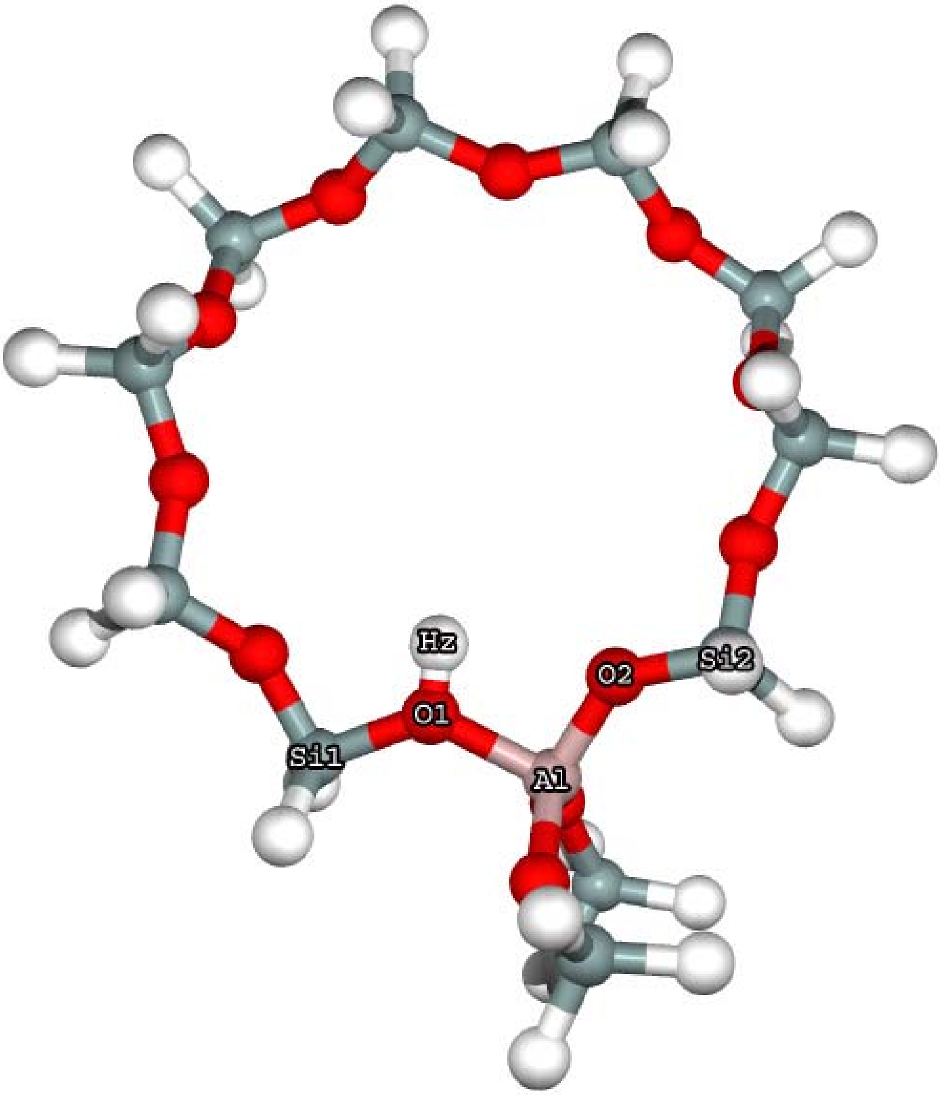

Figure 2

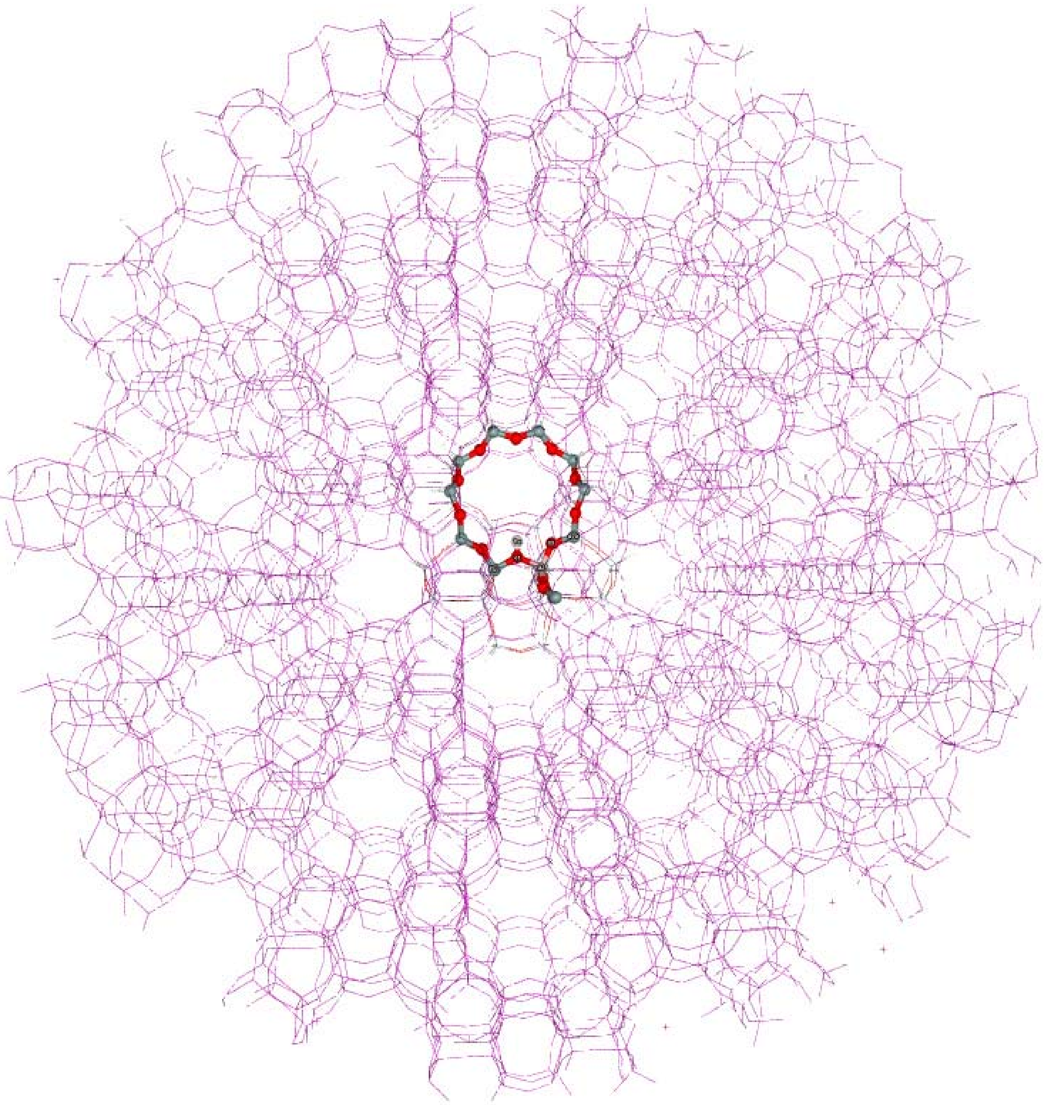

Figure 3

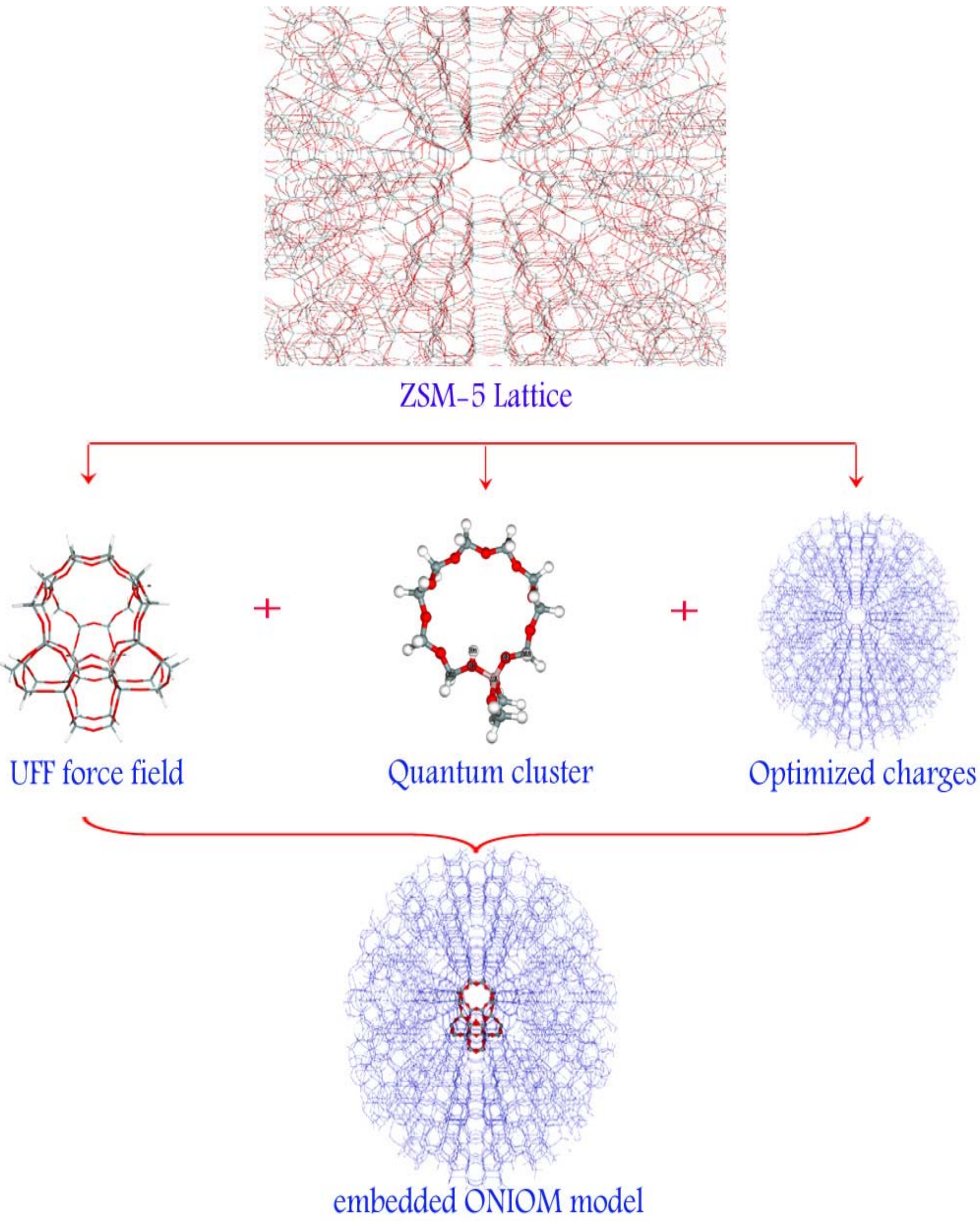

ZSM–5 Lattice
UFF force field
+
Quantum cluster
+
Optimized charges
embedded ONIOM model

Figure 4

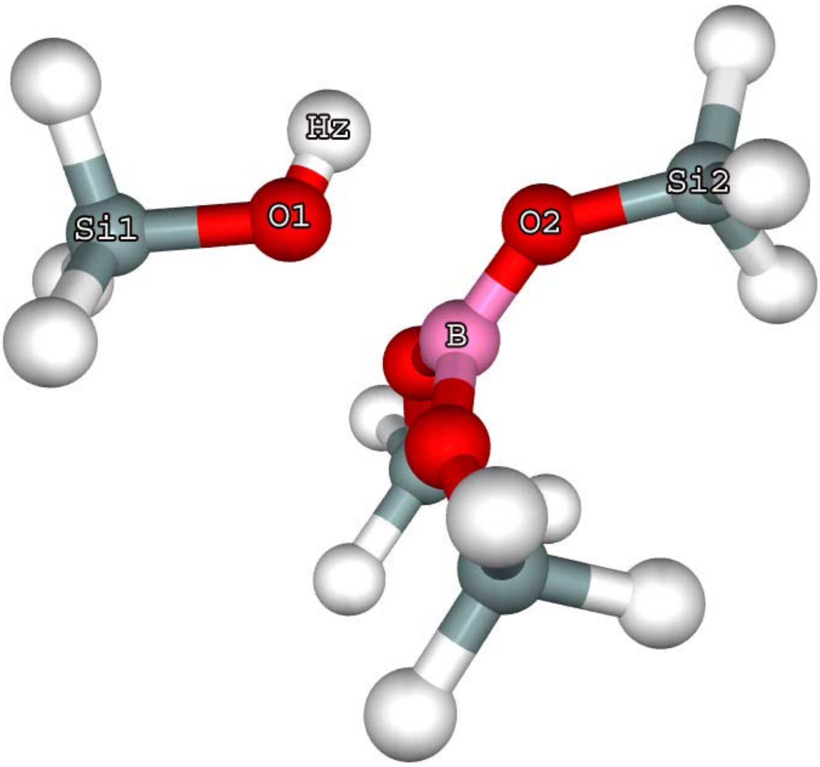

Figure 5

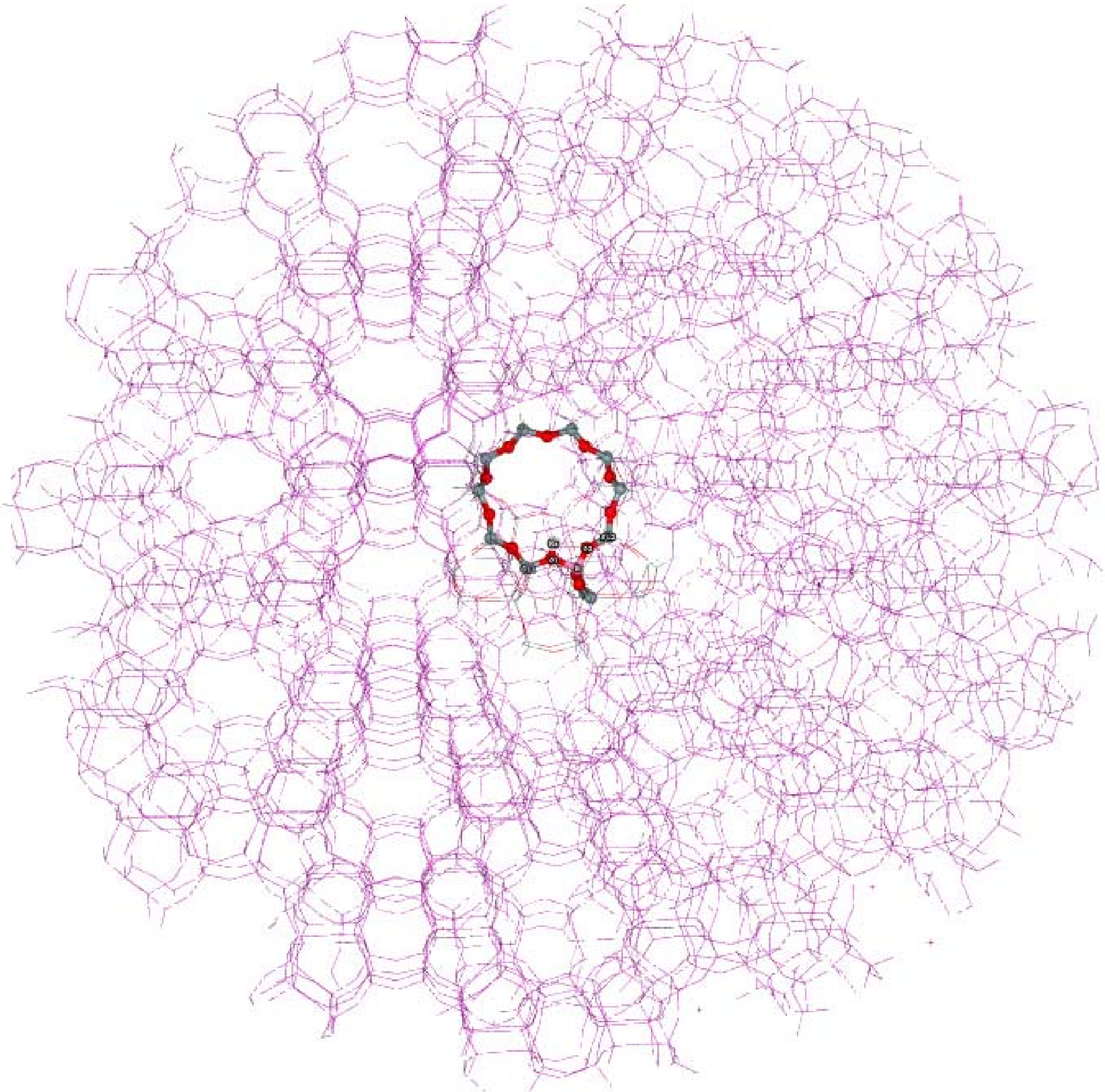

Figure 6

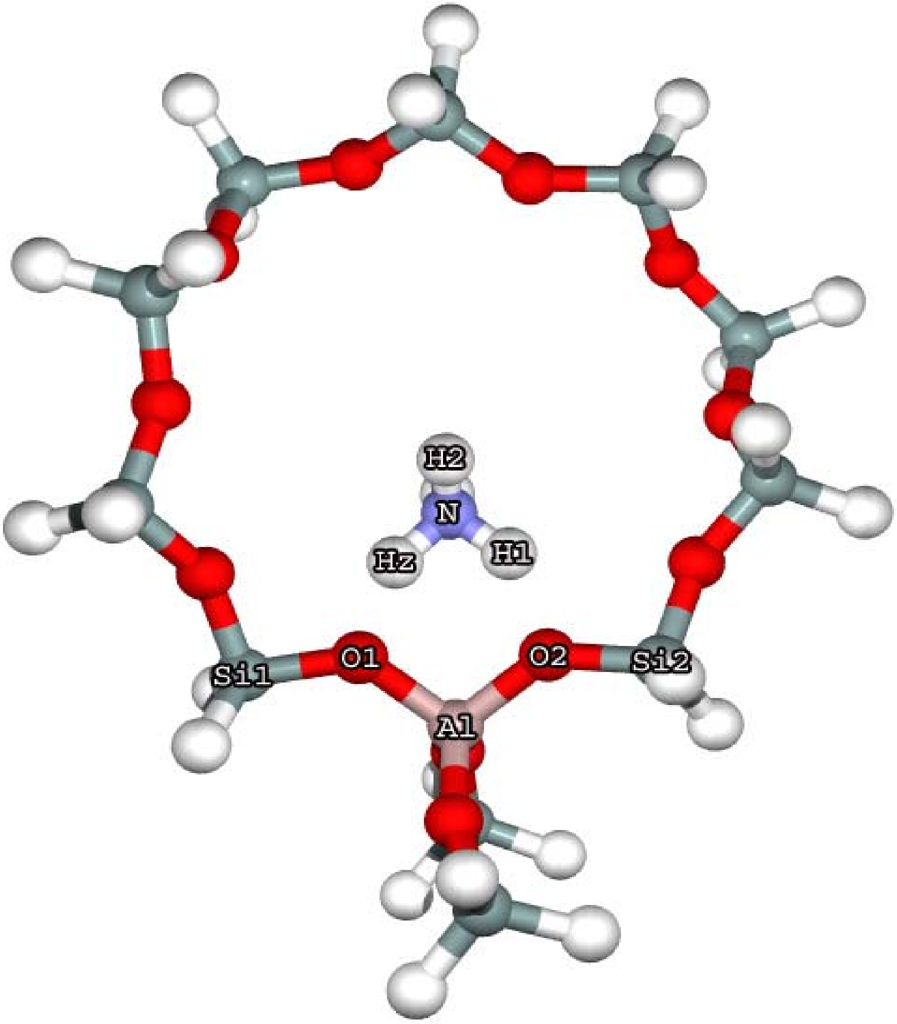

Figure 7

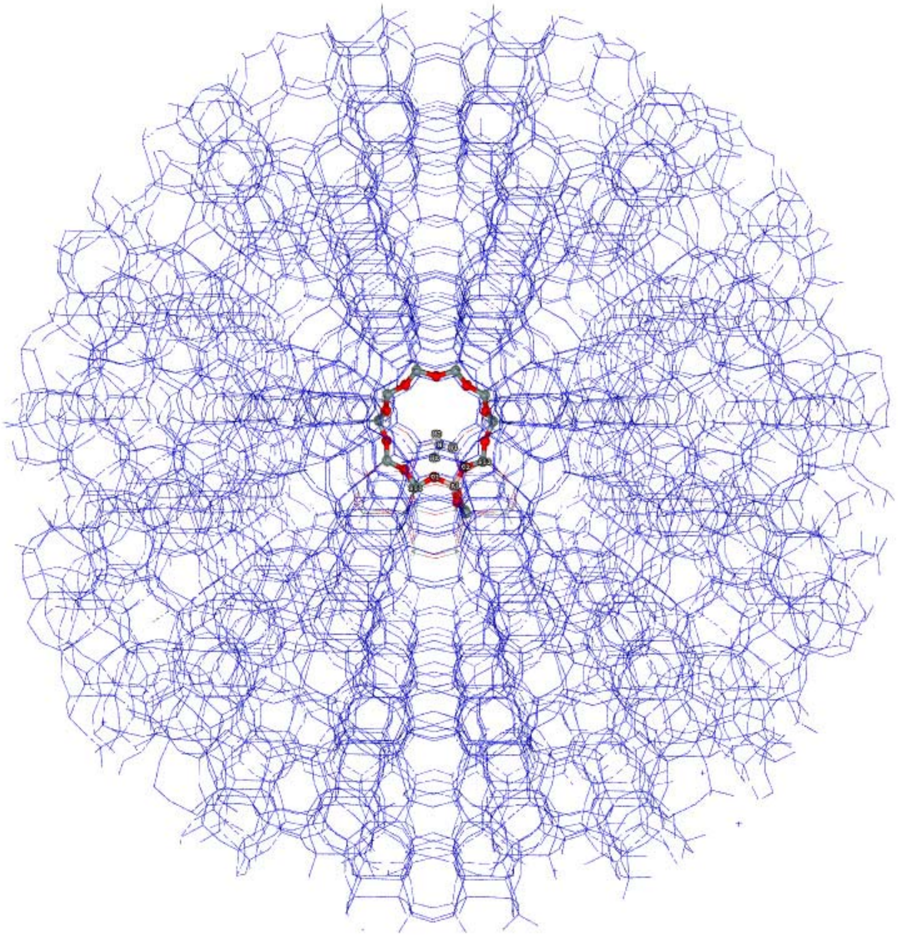

Figure 8

Table 1. The distances of T – O1 in isolated H-ZSM-5 with B3LYP/6-31G (d, p) level of theory.

Level of Theory	**Al – O1**	**B – O1**	**Ga – O1**
5T Cluster	185.60	207.16	193.22
12T Cluster	183.98	204.57	191.61
12T E-ONIOM	179.40	176.88	187.46

Table 2. The distanced of O – H in isolated H-ZSM-5 with B3LYP/6-31G (d, p) level of theory

Level of Theory	**Al**-ZSM-5	**B**-ZSM-5	**Ga**-ZSM-5	acidity
5T Cluster	96.80	96.45	96.83	B < Al < Ga
12T Cluster	96.98	96.66	97.01	B < Al < Ga
12T E-ONIOM	97.07	96.93	97.06	B < Ga < Al
Experimental sequence of acid strength	B-ZSM-5 < Ga-ZSM-5 < Al-ZSM-5			

Table 3 PA and ν_{OH} calculated with B3LYP/6-31G (d, p) level of theory

Model	**PA (kcal/mol)**	
	12T Cluster	**E-ONIOM 12T**
B-ZSM-5	320.12	363.69
Ga-ZSM-5	313.36	362.31
Al-ZSM-5	308.98	357.68
Acidity sequence	B-ZSM-5 < Ga-ZSM-5 < Al-ZSM-5	

Table 4 The distances of O – H_z in isolated H-ZSM-5 with B3LYP/6-31G (d, p) level of theory

Level of Theory	**Al**	**B**	**Ga**	**Acidity trend**
5T Cluster	96.80	96.45	96.83	B < Al < Ga
12T Cluster	96.98	96.66	97.01	B < Al < Ga
12T E-ONIOM	97.08	96.93	97.06	B < Ga < Al
ν_{OH} (cm^{-1}) calculated IR frequency	3604	3616	3608	B < Ga < Al

Table 5 The calculated ν_{OH} with B3LYP/6-31G (d,p) level of theory.

ν_{OH} (cm^{-1})	Acidity trend	Tetrahedral atom		
		Al	**Ga**	**B**
12T E-ONIOM	B < Ga < Al	3604	3608	3616
12T Cluster	B < Al < Ga	3614	3612	3658
ν_{OH} [32] 8T cluster	B < Ga < Al	3816	3825	3830
ν_{OH} from IR [34]	B < Ga < Al	3610	3620	3725

Table 6 Comparisons of Calculated Adsorption Energies of NH_3/Zeolite including BSSE at 6-311++G** basis set with Previous Theoretical and Experimental Results

	Level of Theory	**Cluster**	**Model**	**ΔE**
Al	B3LYP/6-31G (d,p)	12T	E-ONIOM	33.98
Al [33]	B3LYP/3-21G	8T	Cluster	50.7
Al [35]	experiment			33.5 – 35.6
Ga	B3LYP/6-31G (d,p)	12T	E-ONIOM	31.43
Ga [33]	B3LYP/3-21G	8T	Cluster	50.0
Ga [35]	experiment			34.52 – 36.90
B	B3LYP/6-31G (d,p)	12T	E-ONIOM	24.86
B [33]	B3LYP/3-21G	8T	Cluster	41.0